OPEN ACCESS

University of BRISTOL

Dacre, H., Western, L. M., Say, D., O'Doherty, S., Arnold, T., Rennick, C., & Hawkins, E. (2021). Detectability of COVID-19 global emissions reductions in local CO2 concentration measurements. *Environmental Research Letters*, *16*(9), [094043]. https://doi.org/10.1088/1748-9326/ac1eda

Peer reviewed version

License (if available):
CC BY

Link to published version (if available):
10.1088/1748-9326/ac1eda

Link to publication record in Explore Bristol Research
PDF-document

This is the author accepted manuscript (AAM). The final published version (version of record) is available online via IOP Publishing at 10.1088/1748-9326/ac1eda. Please refer to any applicable terms of use of the publisher.

University of Bristol - Explore Bristol Research
General rights

This document is made available in accordance with publisher policies. Please cite only the published version using the reference above. Full terms of use are available:
http://www.bristol.ac.uk/red/research-policy/pure/user-guides/ebr-terms/

Detectability of COVID-19 global emissions reductions in local CO_2 concentration measurements

H F Dacre[1], L M Western[2], D Say[2], S O'Doherty[2], T Arnold[3,4], C Rennick[3] and E Hawkins[5]

[1] University of Reading, Department of Meteorology, Reading, UK
[2] School of Chemistry, University of Bristol, Bristol, UK
[3] National Physical Laboratory, Teddington, Middlesex, UK
[4] School of GeoSciences, University of Edinburgh, Edinburgh, UK
[5] National Centre for Atmospheric Science, Department of Meteorology, University of Reading, Reading, UK

Abstract. It is estimated that global anthropogenic carbon dioxide (CO_2) emissions reduced by up to 12% at the start of 2020 compared to recent years due to the COVID-19 related downturn in economic activity. Despite the large decrease in CO_2 emissions, no reduction in the trend in background atmospheric CO_2 concentrations has been detected. So, how long would it take for sustained COVID-19 CO_2 emission reductions to be detected in daily and monthly averaged local CO_2 concentration measurements? CO_2 concentration measurements for 5 measurement sites in the UK and Ireland are combined with meteorological numerical weather prediction data to build statistical models that can predict future CO_2 concentrations. It is found that 75% of the observed daily variability can be explained by these simple models. Emission reduction scenario experiments using these simple models illustrate that large daily and seasonal variability in local CO_2 concentrations precludes the rapid emergence of a detectable signal. COVID-19 magnitude emissions reductions would only be detectable in the daily CO_2 concentrations after at least 38 months and in monthly CO_2 concentrations after 11 months of sustained reductions. For monthly CO_2 concentrations the time of emergence is similar for all sites since the seasonal variability is largely driven by non-local fluxes of CO_2 between the terrestrial biosphere and the atmosphere. The COVID-19 CO_2 anthropogenic emissions reductions are similar in magnitude to those that are required to meet the Paris Agreement target of keeping global temperatures below 2°C. This study demonstrates that, using measurements alone, there will be a considerable lag between changes in global anthropogenic emissions and a detected signal in local CO_2 concentration trends. Thus, there is likely to be a delay of several years between changes in policy designed to meet CO_2 anthropogenic emissions targets and our ability to detect the impact of these policies on CO_2 concentrations using atmospheric measurements alone.

Keywords: CO2 emissions policy, climate change, multiple linear regression Submitted to: *Environ. Res. Lett.*

1. Introduction

Electricity production, transportation and industrial activity account for more than 80% of CO_2 emissions from fuel combustion (Quadrelli and Peterson, 2007). Since the start of 2020, COVID-19 restrictions have significantly reduced these activities. Current estimates suggest that global fossil fuel CO_2 emissions in 2020 may have dropped by around 7-8% (Hale and Leduc (2020), Le Quere et al. (2020), Liu et al. (2020), Friedlingstein et al. (2020)). Andreoni (2021) estimate that in Europe more than 195,600 thousand tons of CO_2 have been avoided between January and June 2020, compared to the same period of the previous year, representing a -12.1% emissions change. A decline in annual CO_2 emissions of this size would exceed any decline since the end of World War II. The magnitude of these emissions reductions is similar to those required to meet the target of the Paris Agreement, which aims to keep the global temperature rise below 2°C (hereafter 'Paris Agreement magnitude emissions reductions'). To meet the Paris Agreement temperature target, emissions from energy production and transport will have to peak almost immediately in the developed world (Annex I countries) and decline at about 10% each year until net-zero emissions are reached around 2030 (IPCC, 2018). Thus the COVID-19 crisis presents a test bed for understanding these longer-term climate change policies on a more immediate time-scale.

While the recent reductions in CO_2 emissions are indeed substantial, they do not immediately equate to similar reductions in the trend of atmospheric CO_2 concentrations. Background CO_2 concentration measurements have not, so far, shown any changes as a result of COVID-19 emissions reductions (Liu et al. 2020). This is consistent with previous situations when reductions in CO_2 associated with economic downturns did not significantly change the trend in CO_2 concentrations (Granados et al. 2012). The lack of sensitivity to emissions reductions is due to the long atmospheric lifetime of CO_2 (50-200 years) which makes any perturbation in emission rate small compared to the reservoir of CO_2 currently present in the atmosphere. In addition, the large daily and seasonal variability of CO_2 concentrations makes changes in global CO_2 emissions difficult to detect (Samset et al. 2020). Thus if we cannot expect immediately measurable impacts, how long would we need to wait to detect a change in the CO_2 concentration trend due to COVID-19 emission reductions?

In the climate change literature, many studies have investigated the response of the climate system to changes in greenhouse gases (Taylor and Penner 1994, Stainforth et al. 2005, Sitch et al. 2015). These studies typically involve running experiments with coupled atmosphere-ocean climate models with greenhouse gas forcing running over 50-100 year time periods. They may also be coupled to models of other processes in the Earth's atmosphere such as the carbon cycle, so as to better simulate climate feedbacks such as interaction with the terrestrial ecosystems or oceans. On decadal to centennial timescales changes in CO_2 emissions can alter the climate. Therefore, these long integrations are necessary so that the response of the climate to the changing

greenhouse gas emissions can reach equilibrium (Tebaldi and Friedlingstein, 2013). However, on shorter timescales (days to months) CO_2 behaves more like a passive tracer. The concentrations of CO_2 on these timescales is largely controlled by changes in the weather and terrestrial biospheric activity. Therefore complex climate models which represent interactions occurring over longer timescales (years to decades) are not needed to capture the near-term consequence of changes in CO_2 emissions on CO_2 concentrations.

The aim of this work is to determine how long it would take for COVID-19/Paris Agreement magnitude emissions reductions to be detected in local daily and monthly CO_2 concentration measurements. We have built multiple linear regression models, similar to those used to predict short-lived air quality pollutants (e.g. Carslaw and Beevers (2005), Dacre et al. (2020)), to predict CO_2 concentrations using only meteorological data and recent local CO_2 measurements. These models will not capture the responses in the complex models because they are tuned using recent data and they do not include climate feedbacks. However, these reduced complexity models may nevertheless be used to gain insights into our ability to detect greenhouse gas emissions reductions. In addition, they are much less computationally expensive, making them very fast to run.

Table 1. Location, inlet height (metres above ground level, magl) and data availability for the 5 CO_2 measurement sites used in this study.

Site	Lat/Lon	Inlet height (magl)	Data availability
Mace Head	53.327°N, 9.904°W	23	2011 - present
Tacolneston	52.518°N, 1.139°E	185	2012 - present
Ridge Hill	51.998°N, 2.540°W	90	2012 - present
Bilsdale	54.359°N, 1.150°W	248	2014 - present
Heathfield	50.977°N, 0.231°E	100	2013 - present

2. Data

2.1. CO_2 Data

The hourly atmospheric CO_2 measurements used in this study were taken from five in-situ observatories situated across the UK and Ireland (figure 1). Four of these stations, Tacolneston, Ridge Hill, Bilsdale and Heathfield, form the UK-based part of the UK Deriving Emissions linked to Climate Change (DECC) network (Stanley et al., 2018; Stavert et al. 2019). Each of these sites makes use of a tall telecommunications tower to sample air from multiple height inlets (ranging from 42 to 248 meters above ground level (magl) across the network). At each UK DECC site, we use data from the highest

inlet only (Table 1). The fifth site, Mace Head, is situated on the west coast of Ireland. This station is ideally positioned to intercept northern hemispheric background air from the North Atlantic. CO_2 measurements from Mace Head are made by Laboratoire des Sciences du Climat et de l'Environnement (LSCE) as part of the Integrated Carbon Observation System (ICOS) network, from a 23 magl sample inlet (Vardag et al., 2014). Note that lower-frequency CO_2 measurements are available from Mace Head data prior to 2011.

Figure 1 shows the average footprint emissions sensitivity obtained from 30 day backwards simulations of the Met Office's Numerical Atmospheric dispersion Modelling Environment (NAME) model for the five sites for March 2020. The sensitivity is defined as the contribution per unit emission to the mole fraction measurement (Manning et al. 2011). These footprints provide an indication of the location of the local emissions contributing to the measurements at each site in March 2020. At all five sites, continuous in-situ CO_2 measurements are made using cavity ring-down spectrometers (CRDS, Picarro G2301 or G2401). At UK DECC sites, ambient measurements are corrected for linear instrumental drift via daily measurements of a standard gas. A small non-linear correction is applied based on monthly analyses of four calibration gases that span above and below the ambient mole fraction range (Stanley et al., 2018). The calibration strategy differs slightly at Mace Head, where ambient measurements are assigned a mole fraction based on comparison to a linear fit of four calibration cylinders. Like the UK sites, these calibration gases span the complete ambient range. All calibration cylinders are of natural composition and were assigned CO_2 mole fractions at the World Calibration Centre at Empa or the GasLab, Max Planck Institute for Biogeochemistry, Jena, linking them to the World Meteorological Organization (WMO) X2007 CO_2 calibration scale.

2.2. Meteorological Data

The meteorological data to build the statistical models in this study comes from the UK Met Office UKV model (Tang et al. 2013). Hourly data covering the period 1 January 2015 - 31 May 2020 is used. Hourly 4D-Var assimilation allows the production of state-of-the-art weather forecasts for the UK, initialised every hour (Ballard et al. 2016). The UKV has a high resolution inner domain (1.5 km grid spacing) over the UK, separated from a lower resolution grid (4 km grid spacing) near the boundaries by a variable resolution transition zone. The high resolution contains a better representation of land surface processes and orography than coarser resolution global models. Sub-grid scale processes such as, boundary layer turbulence, radiation, cloud, microphysics and orographic drag are represented by parameterizations. The UKV model has been shown to compare well against observations (Lean et al. (2008), Roberts and Lean (2008), Clark et al. (2016)). Meteorological data for the 5-year period (1 January 2015 - 31 December 2019) is extracted from the UKV and interpolated to the location of the DECC sites to build the statistical models described in section 3. One advantage of using

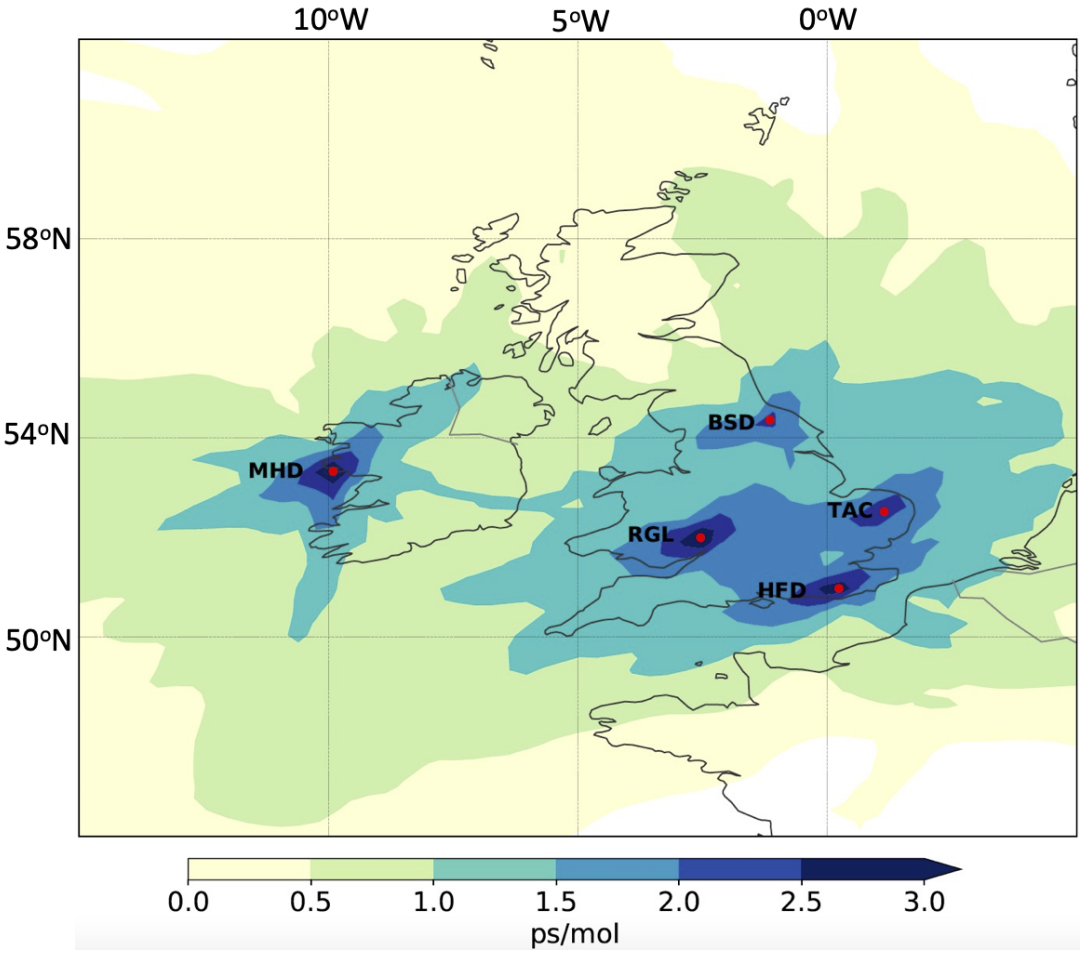

Figure 1. Location of measurement sites used in this study. Mace Head (MHD), Bilsdale (BSD), Ridge Hill (RGH), Heathfield (HFD) and Tacolneston (TAC). Overlaid is the average footprint emissions sensitivity in picoseconds per mole (ps/mol), obtained from 30 day backwards simulations of the Met Office's Numerical Atmospheric dispersion Modelling Environment (NAME) model for the five sites for March 2020.

weather model output is that above surface variables, such as boundary layer height, can be extracted, although modelled boundary layer height has not been evaluated at many sites in the UK due to lack of climatological measurements (Harvey et al. 2013, 2015). One disadvantage of using weather model output is that the resolution of the model data is 1.5 km^2, whereas the CO_2 concentration data are point measurements. If they were available, use of local meteorological measurements to build the statistical models would be more accurate.

3. Multiple Linear Regression Modelling

In order to predict daily and monthly average CO_2 concentrations during the ongoing COVID-19 restrictions, multiple linear regression (MLR) models are built using up to 5-years of DECC and UKV data (2015-2019). MLR modelling is used since the

concentration of CO_2 is likely to depend on more than one predictor variable. The technique enables the relative influences of the predictor variables to be analysed, which allows us to perform the simple CO_2 emission scenario experiments described in section 5. MLR modelling is commonly used for predicting the variability in short-lived pollutant concentrations such as NO_2 (Shi and Harrison (1997); Carslaw and Beevers (2005); Dacre et al. (2020)). The MLR models predict the daily average CO_2 concentrations we would expect, during the COVID-19 period, given no change in CO_2 emissions. Several meteorological and temporal explanatory variables (x_i) are used to predict CO_2 concentrations (y) at each DECC station. The regression coefficients (β_i) describe the size of the effect of the explanatory variable on the daily CO_2 concentrations and α is the value y is predicted to have when all the explanatory variables are equal to zero.

$$y = \sum_{i=1}^{n} \beta_i x_i + \alpha \tag{1}$$

The Akaike Information Criterion (AIC) is used to determine which explanatory variables to include in the models. The model with the lowest AIC score is expected to have the best balance between its ability to fit the data set and its ability to avoid over-fitting the data set. The explanatory variables and regression coefficients used in this study are shown in table 2. Since wind direction is cyclic not linear (i.e. 0 and 360 degrees have the same direction) it is partitioned into its northerly (v-wind) and easterly (u-wind) components. Wind speed, wind direction and temperature are all extracted 10 m above ground level. Sensitivity studies using meteorological variables extracted at the height of the sample inlets for each site did not improve the MLR models.

Our aim in the design of the MLR models was to keep the number of explanatory variables to a minimum and to restrict the models to use local data only. This is desirable to ensure that others, with only local CO_2 concentration and meteorological measurements available to them, can build similar models for their site locations. Also, for simplicity, the same explanatory variables are used for each of 5 sites analysed. The importance of each variable in explaining the observed CO_2 concentrations varies for each site, but the variables in table 2 were found to contribute to a reduced AIC for all 5 sites.

4. Evaluation of predicted CO_2 concentrations

In this section the CO_2 concentrations predicted by the MLR models are compared to the observed CO_2 concentrations at all 5 DECC sites. The evaluation is performed for various temporal averaging periods. The aim is to determine whether the MLR models are a credible representation of reality and thus can be used to perform emission scenario experiments.

Table 2. Regression coefficients (β_i) from the MLR models for each measurement site. The coefficients quantify how much the daily CO_2 concentration is expected to increase/decrease when each explanatory variable (x_i) increases by one, holding all the other variables constant. Explanatory variables are monthly averaged temperature (averaged over the preceding month), daily averaged easterly wind speed (u-wind), daily averaged northerly wind speed (v-wind) and daily averaged boundary layer depth (BLD). Coefficients are only included where they are significant at the 5% level.

Explanatory variable (x_i)		Ridge Hill	Tacolneston	Bilsdale	Mace Head	Heathfield	Average
Date	β_1	0.007	0.007	0.007	0.007	0.007	0.007
Temperature (K)	β_2	-1.1	-1.0	-1.2	-1.5	-1.2	-1.2
U-wind (ms^{-1})	β_3	3.4	1.2	2.4	2.3	1.8	2.2
V-wind (ms^{-1})	β_4	-	-1.1	-0.8	0.7	1.4	0.2
BLD (m)	β_5	-0.004	-0.007	-	-0.002	-0.008	-0.005

4.1. Annual and seasonal CO_2 concentration variability

Figure 2 shows the yearly averaged observed and predicted CO_2 concentrations between January 2015 and June 2020. At all sites there is a monotonic increase in yearly averaged CO_2 concentrations. CO_2 concentrations are primarily rising because of the increased amounts of fossil fuels that humans are burning for energy. The predicted CO_2 concentrations capture this annual increase in CO_2 concentrations due to the inclusion of the date in the MLR models with a coefficient of 0.007 ppm/day at all sites which is equivalent to 2.5 ppm/year (Table 2).

Figure 2 also shows the monthly averaged observed and predicted CO_2 concentrations between January 2015 and June 2020. At all sites there is a strong annual cycle in CO_2 concentrations, with highest CO_2 concentrations measured during the winter months and lowest CO_2 concentrations measured during the summer months. This annual cycle is the result of photosynthetic activity by plants. As plants begin to photosynthesize in the spring and summer, they absorb CO_2 from the atmosphere and eventually use it as a carbon source for growth and reproduction. Once winter arrives, plants save energy by decreasing photosynthesis. Without photosynthesis, the dominant process is the exhalation of CO_2 by the total ecosystem, including bacteria, plants, and animals. The modelled CO_2 concentrations capture the annual cycle in CO_2 concentrations fairly well due to the inclusion of monthly averaged temperature in the MLR models. The coefficients used in the MLR models for monthly averaged temperature are all negative indicating that CO_2 decreases as the temperature increases, and vice-versa, with an average coefficient of -1.2 ppm/K (Table 2).

4.2. Daily CO_2 concentration variability

In this section we focus on the daily variability in CO_2 concentrations, typically caused by the movement of synoptic-scale high and low pressure systems. To illustrate this

we compare the daily averaged observed and predicted CO_2 concentrations between January 2020 and June 2020 (Figure 3). Note that no data from 2020 was used to build the MLR models. The daily variability is largely driven by transport and mixing of CO_2 in the atmospheric boundary layer. High CO_2 concentrations occur when the boundary layer is shallow. During these conditions mixing is suppressed and emissions do not disperse rapidly away from sources but are trapped within the boundary layer where they can accumulate. The MLR models quantify this negative relationship with an average coefficient of -0.005 ppm/m. Since the daily averaged BLD can vary by several hundred metres this can result in CO_2 variability of 1-2 ppm/day. In addition, for certain wind directions, transport from regional CO_2 sources towards the measurement site occurs resulting in high CO_2 concentrations. The coefficients used in the MLR models for easterly wind speeds are all positive. This suggests that easterly winds, which advect air from mainland Europe, contain higher CO_2 concentrations than westerly winds which transport relatively low CO_2 concentration air from the North Atlantic. The coefficients for northerly wind speeds are more mixed. The Tacolneston and Bilsdale MLR models contain negative coefficients indicating that southerly winds increase CO_2 concentrations. This is consistent with their locations which have a long fetch of sea to their north. Conversely, the Heathfield and Mace Head MLR models contain positive coefficients indicating that northerly winds increase CO_2 at these sites. Heathfield is located south of several large urban areas so is potentially influenced by CO_2 emitted locally. Finally, Ridge Hill has no significant correlation with northerly wind direction since there are sources of CO_2 to both the north and south. Thus the modelled CO_2 concentrations capture the daily variability in CO_2 concentrations due to the inclusion of wind speed, wind direction and boundary layer depth in the MLR models.

4.3. MLR model evaluation

Over the training period (Jan 2015- Dec 2019), the MLR models capture 75% of the observed variability in daily averaged CO_2 concentrations with a root mean square error (RMSE) of 3.71 ppm (table 3). The RMSE in daily average CO_2 concentrations is relatively large due to an underestimation of the spikes in the observed daily CO_2 concentrations which are likely to be due to local emissions of CO_2 occurring within a few km's surrounding the tall towers. The normalised mean bias (NMB) is close to zero for all sites. The highest correlations (R^2) and lowest RMSE are found at Mace Head and Bilsdale. These sites have relatively small daily variability compared to the other sites suggesting that they are influenced less by local sources of pollution. Over the 2015-2019 training period the models explain more of the variability in the Spring/Summer ($R^2 = 0.77$) than in the Autumn/Winter periods ($R^2 = 0.68$) and the RMSE is lower (3.36ppm and 4.01ppm respectively) (table 3). This is due to spikes in the observed daily CO_2 concentrations which occur predominantly during the winter and can reach 440ppm (figure 2).

During 2020 the correlations are lower than during the training period but the MLR

models still explain on average 67% of the observed variability in daily CO_2 (table 3). After the 16 March 2020 (UK lockdown) the RMSE increases at 4 out of the 5 sites (figure 3). However, none of the MLR models systematically overestimate the observed CO_2 concentrations after the UK lockdown demonstrating that it will take longer than 2 months for any signal of reduced CO_2 emissions to be observed in the atmospheric CO_2 concentrations.

Table 3. Correlation (R^2), root mean square error (RMSE) and normalised mean bias (NMB) statistics for daily model prediction of CO_2 concentration at each measurement site. Statistics are calculated for the model training period (January 2015- December 2019), Autumn/Winter months (September-February) in the training period, Spring/Summer months (March-August) in the training period and for the prediction period (January - December 2020).

	Ridge Hill	Tacolneston	Bilsdale	Mace Head	Heathfield	Average
2015-2019						
R^2	0.75	0.71	0.79	0.78	0.73	0.75
RMSE (ppm)	3.77	3.95	3.32	3.21	4.28	3.71
NMB (%)	-0.02	0.01	0.01	-0.01	-0.003	0.00
Autumn/Winter						
R^2	0.71	0.57	0.71	0.76	0.63	0.68
RMSE (ppm)	3.94	4.53	3.55	3.10	4.94	4.01
NMB (%)	0.04	-0.05	0.00	0.10	-0.03	0.01
Spring/Summer						
R^2	0.76	0.74	0.79	0.79	0.75	0.77
RMSE (ppm)	3.43	3.36	3.11	3.23	3.68	3.36
NMB (%)	-0.07	0.08	-0.02	-0.09	0.04	-0.01
2020						
R^2	0.62	0.65	0.75	0.68	0.65	0.67
RMSE (ppm)	3.52	3.81	2.96	2.97	4.03	3.46
NMB (%)	-0.03	-0.15	0.05	-0.01	0.03	-0.02

5. Global CO_2 emission scenarios

Since the MLR models describe so much of the observed daily CO_2 variability they provide a realistic substitute for the real world and thus can be used to perform emission scenario simulations. In particular, the MLR models are used in this section to determine how long it would take for COVID-19/Paris Agreement magnitude CO_2 emissions reductions to be detected in daily and monthly averaged CO_2 measurements. Since CO_2 has a lifetime much longer than 5 years, simple global emission scenario simulations can be performed by scaling the regression coefficient controlling the trend (i.e. the date) whilst maintaining the seasonal and daily variability. $\beta_1 = 0.007$ ppm/day represents 100% of the annual CO_2 concentration increase due to increasing anthropogenic emissions and $\beta_1 = 0.0$ ppm/day represents net-zero anthropogenic

emissions. Thus sensitivity to different global emission scenarios can be performed while keeping the seasonal and daily variability constant (i.e. the regression coefficients for wind speed and wind direction, boundary layer depth and monthly averaged temperature remain unchanged) .

The variability in daily CO_2 concentrations (daily noise) is estimated by the standard deviation of observed CO_2 concentrations over 30-day moving windows (figure 4). The variability in monthly CO_2 concentrations (monthly noise) is estimated by the standard deviation of the 2015-2019 de-trended observed CO_2 concentrations over moving 3 month periods. The difference in simulated CO_2 concentration between the 100% emissions and reduced global emissions scenarios (signal) increases with time and is proportional to the magnitude of the global emission reduction. The signal-to-noise ratio thus determines how reductions in CO_2 concentrations resulting from the emissions reduction scenarios compare to the estimated variability in CO_2 concentrations. The time of emergence is defined as the earliest time that the signal-to-noise ratio exceeds a value of 1. Since the time of emergence may depend on the initial conditions it is calculated for simulations initialised at varying weekly intervals between January 2015 and January 2020 to give a range of emergence times for each emission scenario. Figure 4 shows the evolution of daily CO_2 concentrations and daily noise for Ridge Hill assuming 100% emissions (plotted every 7 days). Different emission scenarios are also shown for 2 sites. For the Ridge Hill simulation initialised on 15 January 2015 (Figure 4(a)) the time of emergence for the net-zero scenario simulation (-100%) occurs 10.3 months after the start of the simulation. The time of emergence for the -50%, -25% and -12% emissions scenarios occur 15.3, 27.3 and 50.6 months after the start of the simulation respectively. Figure 4(b) shows simulations initialised at the same time for the Mace Head site. The time of emergence for the net-zero scenario is similar to that at Ridge Hill, for this initialisation time, but the time of emergence for the -50%, -25% and -12% emissions scenarios occurs earlier than the respective emission scenarios at Ridge Hill.

Table 4 shows the range of time of emergence for multiple emission scenarios initialised at monthly intervals. If net-zero anthropogenic emissions are assumed (-100%) then a signal would be detectable in the daily CO_2 concentrations after an average of 8 months. The signal in daily CO_2 concentrations would likely emerge at Bilsdale and Mace Head 2-3 months earlier than the other DECC sites as the daily variability at these sites is smaller than at the other DECC measurement locations. The longest daily time of emergence for the net-zero emission scenario would likely be at the Heathfield site, which is a semi-rural UK site located 19 km south of Royal Tunbridge Wells (population 118,000), in East Sussex, UK. As the emission scenario reduces in magnitude, the daily time of emergence increases. If a 50% reduction in anthropogenic emissions is maintained indefinitely a reduction in the trend of daily CO_2 concentrations would be observable after an average of 15 months. For COVID-19/Paris Agreement like magnitude emissions reductions of -12% (Andreoni 2021) the daily time of emergence would be on average after 38 months. Thus we would be able to detect

a reduction in daily CO_2 concentrations after 2-3 years depending on the measurement site. Note that for the smallest emission reduction scenario (-12% emissions) there are large daily time of emergence inter-quartile ranges due to a decrease in the sample size.

If we average the daily data to calculate monthly CO_2 concentrations then we smooth out the daily variability. Thus we can detect a reduction in the monthly CO_2 concentration trend due to COVID-19 like magnitude emissions reductions earlier, after about 11 months. Therefore, if current global lockdown restrictions continue we might detect a reduction in monthly averaged CO_2 concentration trend some time in 2021 at the earliest. When averaging over a month, the differences in the time of emergence between the measurement sites reduces as the CO_2 concentrations are less dependent on local emissions and are largely driven by non-local biogenic emissions.

Table 4. Time of emergence (ToE, months) of CO_2 concentration differences due to reduced emission scenarios. The ranges are the 25-75th percentile ToE estimated using different start dates and for two averaging periods (24 hours and 30 days).

	Ridge Hill	Tacolneston	Bilsdale	Mace Head	Heathfield	Average
Daily ToE						
-12% emissions	42-48	20-31	32-48	29-37	47-61	38
-25% emissions	24-30	17-28	18-26	17-20	37-41	24
-50% emissions	14-19	12-18	11-15	8-14	19-24	15
-100% emissions	8-12	7-10	6-9	6-8	10-13	8
Monthly ToE						
-12% emissions	8-13	9-15	6-14	8-13	7-15	11
-25% emissions	5-10	6-12	5-10	5-9	5-11	8
-50% emissions	4-8	5-9	4-8	4-8	4-8	6
-100% emissions	3-6	3-6	3-6	3-7	3-6	5

6. Conclusions

In this paper, analysis of 5 CO_2 monitoring sites in the UK and Ireland has shown that after several months of CO_2 emissions reductions there are no detectable decreases in CO_2 concentrations exceeding the natural variations in measured CO_2 concentrations. Furthermore, global emission reduction scenario experiments show that it would take around 3 years of sustained global emissions reductions before any such signal could be detected in the local daily CO_2 concentration trend and 1 year before a reduction in CO_2 concentration trend would be detectable in the monthly averaged local CO_2 concentration trend. Future work could include performing the linear regression modelling using the fossil fuel contribution of CO_2 calculated from the measured ^{14}C content of CO_2, instead of using total CO_2 concentrations. Since the method used to create the MLR models is generalizable, similar MLR models could be built for other locations with only local CO_2 and meteorological measurements available. It would be interesting to perform a similar study at a remote location, such as the Mauna Loa

observatory, which is not affected by local CO_2 emissions in order to determine if the time of emergence appears earlier or later than those estimated for the sites in the UK and Ireland. The models used to make these estimates do not include climate feedbacks or processes determining plant growth which may make any detection of any signal even more difficult, hence these results should be seen as a lower limit. The results of this study show that the growth rate of CO_2 in the atmosphere will not decrease unless there is a substantial and persistent reduction in emissions over many decades.

Since CO_2 emissions are projected to eventually return to business-as-usual levels, the overall impact of COVID-19 CO_2 emission reductions on CO_2 concentrations in the atmosphere and therefore on climate change is likely to be small in the long run. The COVID-19 CO_2 emission reductions are similar in magnitude to those that are necessary to mitigate the worst effects of climate change. The COVID-19 crisis thus offers insights into the substantial changes in behaviour and infrastructure that are necessary if we are to achieve the temperature targets set out by the Paris Agreement. However, the measures deployed in response to the COVID-19 pandemic are not suitable or sustainable in the long term. These results support the need to create policies for recovering from the current economic downturn that do not further increase CO_2 emissions but which provide sustainable growth such as those outlined by Hepburn et al. (2020).

The simple linear regression models used in this study could be used in the future to detect global scale emissions changes. However, the results of this study demonstrate that, using local measurements alone, there will be a significant delay between changes in global emissions and a detected signal in the local CO_2 concentrations.

7. Acknowledgements

The UK DECC network operations were funded by the UK Department of Business, Energy and Industrial Strategy (BEIS) through contract 1537/06/2018 to the University of Bristol. The authors would like to thank Kieran Stanley, Dickon Young, Ann Stavert, Aoife Grant and Anita Ganesan at the University of Bristol for setting up and running the DECC measurement sites. We would also like to thank Dr Adam Wisher, the specialist technician at Tacolneston, for maintaining the instrument. The Mace Head data is provided by ICOS. Maintenance of the Heathfield site measurements is supported by UK National Measurement System funding to the National Physical Laboratory. H.F.Dacre is funded by the NERC Detection and Attribution of Regional greenhouse gas Emissions in the UK (DARE-UK) project NE/S004505/1.

8. Data Availability

CO_2 data from the UK DECC network are available from the Centre for Environmental Data Analysis (CEDA) data archive (https://catalogue.ceda.ac.uk/uuid/a18f43456c364789aac726ed365e41d1). Atmospheric CO2 data from Mace Head is

available at the ICOS Carbon Portal (https://www.icos-cp.eu/): doi:10.18160/ere9-9d85.

9. References

Andreoni, V., 2021. Estimating the European CO2 emissions change due to COVID-19 restrictions. Science of The Total Environment, 769, p.145115.

Ballard, S.P., Li, Z., Simonin, D. and Caron, J.F., 2016. Performance of 4D-Var NWP-based nowcasting of precipitation at the Met Office for summer 2012. Quarterly Journal of the Royal Meteorological Society, 142(694), pp.472-487.

Carslaw, D.C. and Beevers, S.D., 2005. Development of an urban inventory for road transport emissions of NO2 and comparison with estimates derived from ambient measurements. Atmospheric Environment, 39(11), pp.2049-2059.

Clark, P., Roberts, N., Lean, H., Ballard, S.P. and Charlton-Perez, C., 2016. Convection-permitting models: a step-change in rainfall forecasting. Meteorological Applications, 23(2), pp.165-181.

Dacre, H.F., Mortimer, A.H. and Neal, L.S., 2020. How have surface NO2 concentrations changed as a result of the UK's COVID-19 travel restrictions?. Environmental Research Letters. doi.org/10.1088/1748-9326/abb6a2

DECC, 2020. Deriving Emissions linked to Climate Change(DECC) Network. `http://data.ceda.ac.uk/badc/uk-decc-network` [Accessed April 2020]

Diffenbaugh, N.S., Field, C.B., Appel, E.A., Azevedo, I.L., Baldocchi, D.D., Burke, M., Burney, J.A., Ciais, P., Davis, S.J., Fiore, A.M. and Fletcher, S.M., 2020. The COVID-19 lockdowns: a window into the Earth System. Nature Reviews Earth and Environment, pp.1-12.

Forster, P.M., Forster, H.I., Evans, M.J., Gidden, M.J., Jones, C.D., Keller, C.A., Lamboll, R.D., Le Quéré, C., Rogelj, J., Rosen, D. and Schleussner, C.F., 2020. Current and future global climate impacts resulting from COVID-19. Nature Climate Change, pp.1-7.

Friedlingstein, P., O'Sullivan, M., Jones, M. W., Andrew, R. M., Hauck, J., Olsen, A., Peters, G. P., Peters, W., Pongratz, J., Sitch, S., Le Quéré, C., Canadell, J. G., Ciais, P., Jackson, R. B., Alin, S., Aragão, L. E. O. C., Arneth, A., Arora, V., Bates, N. R., Becker, M., Benoit-Cattin, A., Bittig, H. C., Bopp, L., Bultan, S., Chandra, N., Chevallier, F., Chini, L. P., Evans, W., Florentie, L., Forster, P. M., Gasser, T.,

Gehlen, M., Gilfillan, D., Gkritzalis, T., Gregor, L., Gruber, N., Harris, I., Hartung, K., Haverd, V., Houghton, R. A., Ilyina, T., Jain, A. K., Joetzjer, E., Kadono, K., Kato, E., Kitidis, V., Korsbakken, J. I., Landschützer, P., Lefèvre, N., Lenton, A., Lienert, S., Liu, Z., Lombardozzi, D., Marland, G., Metzl, N., Munro, D. R., Nabel, J. E. M. S., Nakaoka, S.-I., Niwa, Y., O'Brien, K., Ono, T., Palmer, P. I., Pierrot, D., Poulter, B., Resplandy, L., Robertson, E., Rödenbeck, C., Schwinger, J., Séférian, R., Skjelvan, I., Smith, A. J. P., Sutton, A. J., Tanhua, T., Tans, P. P., Tian, H., Tilbrook, B., van der Werf, G., Vuichard, N., Walker, A. P., Wanninkhof, R., Watson, A. J., Willis, D., Wiltshire, A. J., Yuan, W., Yue, X., and Zaehle, S.: Global Carbon Budget 2020, Earth Syst. Sci. Data, 12, 3269–3340, https://doi.org/10.5194/essd-12-3269-2020, 2020.

Granados, J.A.T., Ionides, E.L. and Carpintero, Ó., 2012. Climate change and the world economy: short-run determinants of atmospheric CO2. Environmental Science and Policy, 21, pp.50-62.

Hale, G. and Leduc, S., 2020. COVID-19 and CO2. FRBSF Economic Letter, 2020(18), pp.1-06.

Han, P., Cai, Q., Oda, T., Zeng, N., Shan, Y., Lin, X. and Liu, D., 2020. Assessing the recent impact of COVID-19 on carbon emissions from China using domestic economic data. Science of the Total Environment, 750, p.141688.

Hepburn, C., O'Callaghan, B., Stern, N., Stiglitz, J. and Zenghelis, D., 2020. Will COVID-19 fiscal recovery packages accelerate or retard progress on climate change?. Oxford Review of Economic Policy, 36.

Harvey, N.J., Hogan, R.J. and Dacre, H.F., 2013. A method to diagnose boundary-layer type using Doppler lidar. Quarterly Journal of the Royal Meteorological Society, 139(676), pp.1681-1693.

Harvey, N.J., Hogan, R.J. and Dacre, H.F., 2015. Evaluation of boundary-layer type in a weather forecast model utilizing long-term Doppler lidar observations. Quarterly Journal of the Royal Meteorological Society, 141(689), pp.1345-1353.

IPCC, 2018: Summary for Policymakers. In: Global Warming of 1.5°C. An IPCC Special Report on the impacts of global warming of 1.5°C above pre-industrial levels and related global greenhouse gas emission pathways, in the context of strengthening the global response to the threat of climate change, sustainable development, and efforts to eradicate poverty [Masson-Delmotte, V., P. Zhai, H.-O. Pörtner, D. Roberts, J. Skea, P.R. Shukla, A. Pirani, W. Moufouma-Okia, C. Péan, R. Pidcock, S. Connors, J.B.R. Matthews, Y. Chen, X. Zhou, M.I. Gomis, E. Lonnoy, T. Maycock, M. Tignor, and T. Waterfield (eds.)]. World Meteorological Organization, Geneva, Switzerland, 32 pp.

Lean, H.W., Clark, P.A., Dixon, M., Roberts, N.M., Fitch, A., Forbes, R. and Halliwell, C., 2008. Characteristics of high-resolution versions of the Met Office Unified Model for forecasting convection over the United Kingdom. Monthly Weather Review, 136(9), pp.3408-3424.

Le Quéré, C., Jackson, R.B., Jones, M.W., Smith, A.J., Abernethy, S., Andrew, R.M., De-Gol, A.J., Willis, D.R., Shan, Y., Canadell, J.G. and Friedlingstein, P., 2020. Temporary reduction in daily global CO 2 emissions during the COVID-19 forced confinement. Nature Climate Change, 10(7), pp.647-653.

Liu, Z., Deng, Z., Ciais, P., Lei, R., Feng, S., Davis, S.J., Wang, Y., Yue, X., Lei, Y., Zhou, H. and Cai, Z., 2020. COVID-19 causes record decline in global CO2 emissions. Preprint at http://arxiv.org/abs/2004.13614 (2020).

Manning, A.J., O'Doherty, S., Jones, A.R., Simmonds, P.G. and Derwent, R.G., 2011. Estimating UK methane and nitrous oxide emissions from 1990 to 2007 using an inversion modeling approach. Journal of Geophysical Research: Atmospheres, 116(D2).

Marotzke, J. and Forster, P.M., 2015. Forcing, feedback and internal variability in global temperature trends. Nature, 517(7536), pp.565-570.

Mitra, A., Ray Chadhuri, T., Mitra, A., Pramanick, P. and Zaman, S., 2020. Impact of COVID-19 related shutdown on atmospheric carbon dioxide level in the city of Kolkata. Parana Journal of Science and Education, 6(3), pp.84-92.

Roberts, N.M. and Lean, H.W., 2008. Scale-selective verification of rainfall accumulations from high-resolution forecasts of convective events. Monthly Weather Review, 136(1), pp.78-97.

Samset, B.H., Fuglestvedt, J.S. and Lund, M.T., 2020. Delayed emergence of a global temperature response after emission mitigation. Nature communications, 11(1), pp.1-10.

Santer, B.D., Taylor, K.E., Wigley, T.M., Penner, J.E., Jones, P.D. and Cubasch, U., 1995. Towards the detection and attribution of an anthropogenic effect on climate. Climate Dynamics, 12(2), pp.77-100.

Shi, J.P. and Harrison, R.M., 1997. Regression modelling of hourly NOx and NO2 concentrations in urban air in London. Atmospheric Environment, 31(24), pp.4081-4094.

Sitch, S., Friedlingstein, P., Gruber, N., Jones, S. D., Murray-Tortarolo, G.,

Ahlström, A., Doney, S. C., Graven, H., Heinze, C., Huntingford, C., Levis, S., Levy, P. E., Lomas, M., Poulter, B., Viovy, N., Zaehle, S., Zeng, N., Arneth, A., Bonan, G., Bopp, L., Canadell, J. G., Chevallier, F., Ciais, P., Ellis, R., Gloor, M., Peylin, P., Piao, S. L., Le Quéré, C., Smith, B., Zhu, Z., and Myneni, R.: Recent trends and drivers of regional sources and sinks of carbon dioxide, Biogeosciences, 12, 653–679, https://doi.org/10.5194/bg-12-653-2015, 2015.

Stainforth, D.A., Aina, T., Christensen, C., Collins, M., Faull, N., Frame, D.J., Kettleborough, J.A., Knight, S., Martin, A., Murphy, J.M. and Piani, C., 2005. Uncertainty in predictions of the climate response to rising levels of greenhouse gases. Nature, 433(7024), pp.403-406.

Stanley, K.M., Grant, A., O'Doherty, S., Young, D., Manning, A.J., Stavert, A.R., Spain, T.G., Salameh, P.K., Harth, C.M., Simmonds, P.G. and Sturges, W.T., 2018. Greenhouse gas measurements from a UK network of tall towers: technical description and first results. Atmospheric Measurement Techniques, 11(3), pp.1437-1458.

Stavert, A.R., O'Doherty, S., Stanley, K., Young, D., Manning, A.J., Lunt, M.F., Rennick, C. and Arnold, T., 2019. UK greenhouse gas measurements at two new tall towers for aiding emissions verification. Atmospheric Measurement Techniques, 12(8), pp.4495-4518.

Taylor, K.E. and Penner, J.E., 1994. Response of the climate system to atmospheric aerosols and greenhouse gases. Nature, 369(6483), pp.734-737.

Tang, Y., Lean, H.W. and Bornemann, J., 2013. The benefits of the Met Office variable resolution NWP model for forecasting convection. Meteorological Applications, 20(4), pp.417-426.

Tebaldi, C. and Friedlingstein, P., 2013. Delayed detection of climate mitigation benefits due to climate inertia and variability. Proceedings of the National Academy of Sciences, 110(43), pp.17229-17234.

Quadrelli, R. and Peterson, S., 2007. The energy–climate challenge: Recent trends in CO2 emissions from fuel combustion. Energy policy, 35(11), pp.5938-5952.

Vardag, S.N., Hammer, S., O'Doherty, S., Spain, T.G., Wastine, B., Jordan, A. and Levin, I., 2014. Comparisons of continuous atmospheric CH4, CO2 and N2O measurements–results from a travelling instrument campaign at Mace Head. Atmospheric Chemistry and Physics, 14(16), pp.8403-8418.

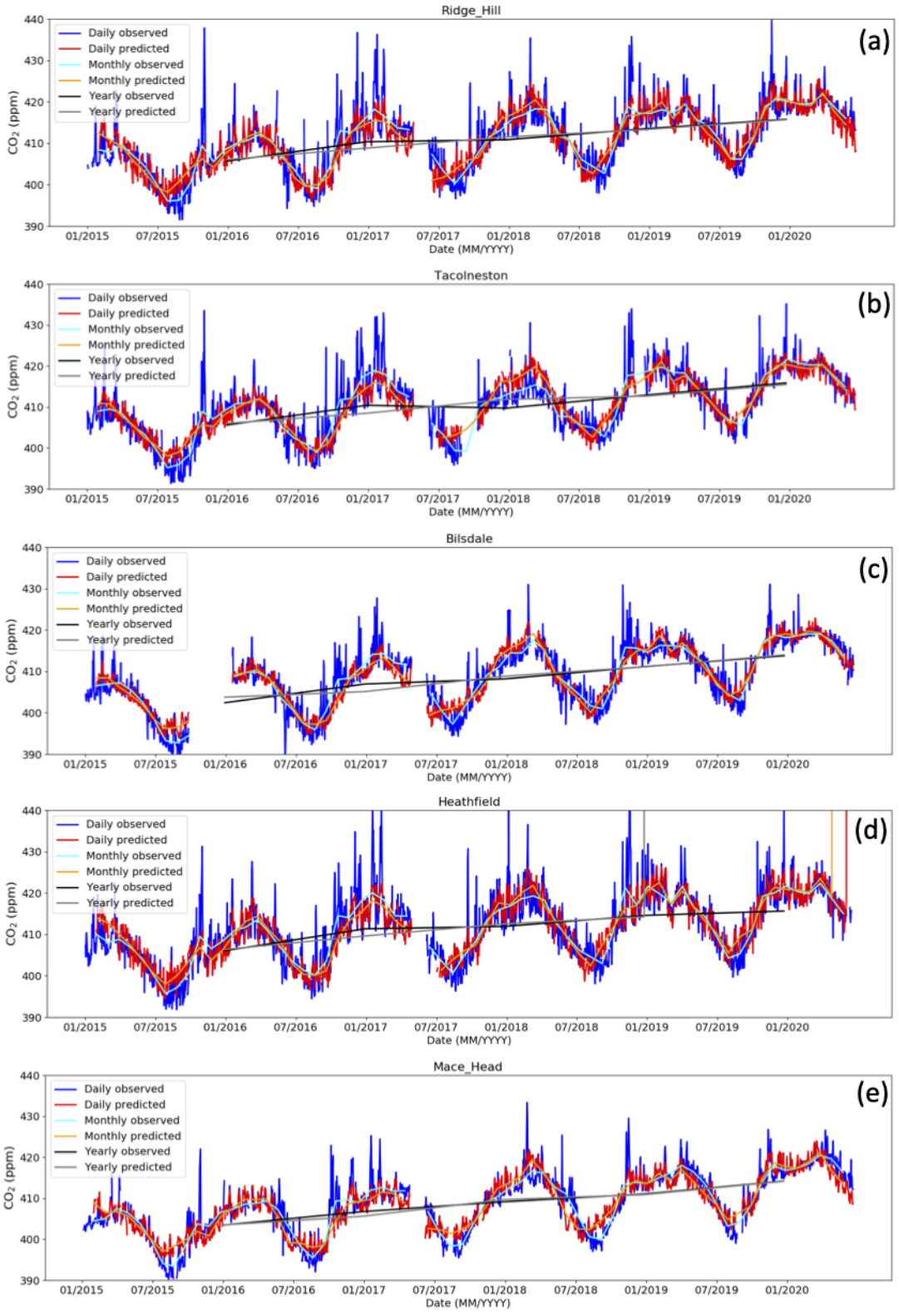

Figure 2. CO_2 concentrations from 1 January 2015 to 30 May 2020 at (a) Ridge Hill, (b) Tacolneston, (c) Bilsdale, (d) Heathfield and (e) Mace Head. Daily averaged observed concentrations (blue) and predicted concentrations (red). 30-day averaged observed concentrations (cyan) and predicted concentrations (orange). Annually averaged observed concentrations (black) and predicted concentrations (grey). Note that there is 2 weeks of missing meteorological data between in 2017.

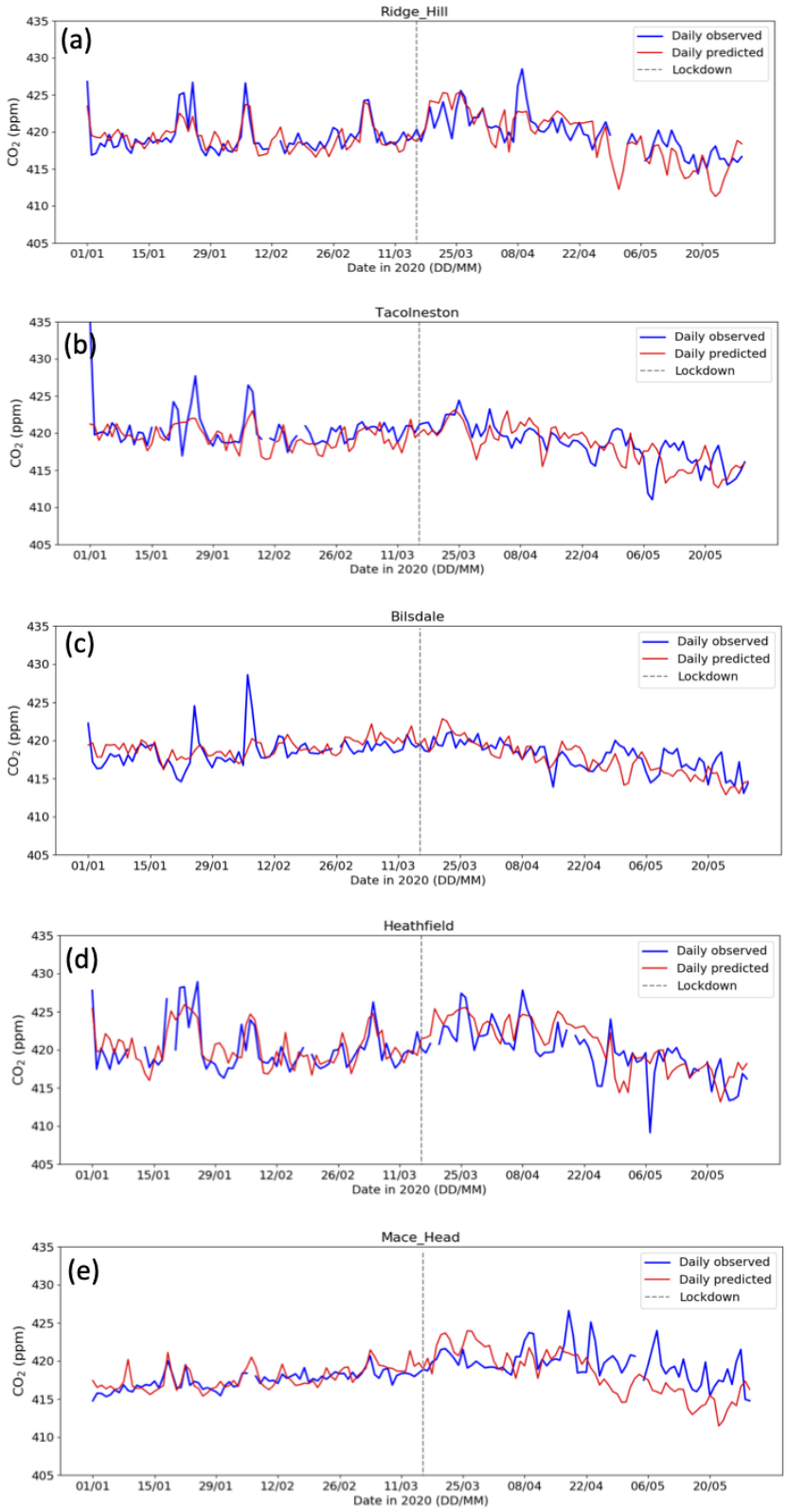

Figure 3. CO_2 concentrations from 1 January - 30 May 2020 at (a) Ridge Hill, (b) Tacolneston, (c) Bilsdale, (d) Ridge Hill and (e) Mace Head. Daily average observed CO_2 concentrations (blue) and modelled CO_2 concentrations (red). Dashed line indicates date of UK lockdown on 16 March 2020.

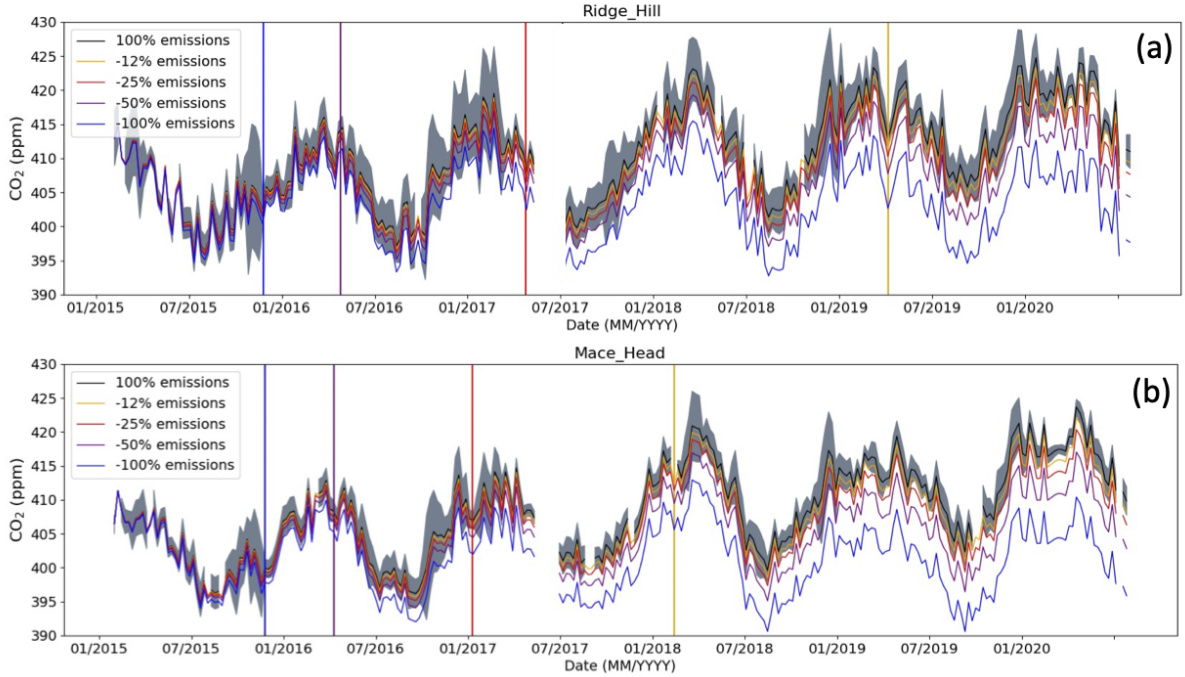

Figure 4. Example 24-hour averaged predicted CO_2 concentrations for the (a) Ridge Hill and (b) Mace Head site with 100% emissions (black), -12% emissions (orange), -25% emissions (red), -50% emissions (purple) and -100% emissions (blue). Grey shading shows 100% emissions simulations ±1 standard deviation of the 24-hour averaged observed CO_2 concentrations for a centred 30-day window. Simulations initialised on 15 January 2015. Vertical lines show the time at which signal-to-noise ratio exceeds 1 (time of emergence) for the different emission scenarios.